

# SIMULATION STUDIES ON THE VERTICAL EMITTANCE GROWTH AT THE EXISTING ATF EXTRACTION BEAMLINE\*

F. Zhou<sup>+</sup>, J. Amann, S. Seletskiy, A. Seryi, C. M. Spencer, M. D. Woodley  
SLAC, Menlo Park, CA 94025, USA

## Abstract

Significant beam intensity-dependence of the vertical emittance growth was experimentally observed at the Accelerator Test Facility (ATF) at KEK extraction beamline. This paper presents the simulations of possible vertical emittance growth sources, particularly in the extraction channel, where the magnets are shared by both the ATF extraction beamline and its damping ring. The vertical emittance growth is observed in the simulations by changing the beam orbit in the extraction channel, even with all optics corrections. The possible reasons for the experimentally observed dependence of the vertical emittance growth on the beam intensity are also discussed. An experiment to measure the emittance versus beam orbit at the existing ATF extraction beamline is ongoing led by the European colleagues.

## MULTIPOLE FIELD ANALYSIS

A small vertical emittance was experimentally achieved in the ATF/KEK damping ring [1]. However, significant dependence of the vertical emittance growth on the beam intensity was observed [2-3] at the ATF extraction beamline when the beam was extracted from the damping ring. Magnets in the extraction channel, such as QM7R and BS1X [4], shared by both the extraction beamline and the damping ring, are probably one of major nonlinear magnetic field sources that create the emittance growth. The extracted beam has a nominal horizontal deviation from the magnet centers, 0.022 m for QM7R and 0.0855 m for BS1X, and the magnetic fields of both magnets are modeled with the 2-D Poisson program [5]. Fig. 1 shows the 1/8<sup>th</sup> of QM7R and the locations of both extracted and stored beams. The magnetic field multipoles are decomposed with respect to the nominal position of the extracted-beam (0.022 m of horizontal offset from the magnet center for QM7R) using the following equation:

$$B_y + jB_x = B_0 \sum_{n=0}^{\infty} b_n (x + jy)^n, \text{ where } B_y \text{ and } B_x \text{ are the}$$

magnetic field components in y- and x-plane, respectively,  $j$  is the imaginary number,  $B_0$  is the normalization constant and  $b_n$  is called the  $2(n+1)$ <sup>th</sup> multipole coefficient. A MathCAD-based built-in function is used to fit the 2-D Poisson-simulated field of QM7R,  $B_x$  and  $B_y$ , as shown in Fig. 2. It is shown that the fitting for the magnetic field multipoles is very well, as explained in detail in the figure caption. The details of the field calculation and its fitting for BS1X are described in Ref. [4]. The corresponding multipole parameters

$$K_n L = \frac{L}{B\rho} \frac{\partial^n B_y}{\partial x^n} \quad (L \text{ is the magnet length and } B\rho \text{ is the}$$

magnetic rigidity) for the QM7R and BS1X are calculated, as given in Table I. It is shown that the sextupoles and octupoles in the QM7R are much stronger than the ones in the BS1X.

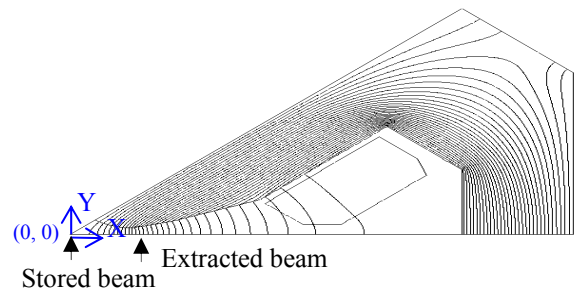


Figure 1: 1/8<sup>th</sup> of the QM7R quad modeled with the Poisson program; the extracted beam is located at  $X=0.022$  m from the magnet center and at  $Y=0$ , and the stored beam is at the magnet center,  $X=0$  and  $Y=0$ .

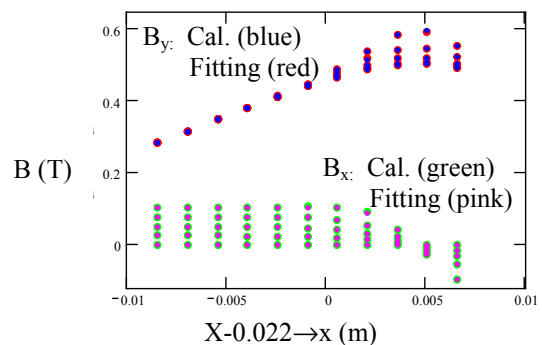


Figure 2: QM7R magnetic field mapping for  $B_y$  and  $B_x$  in the new coordinate system  $x=X-0.022$  and  $y=Y$ . At each  $x$  position, both  $B_x$  and  $B_y$  have five field values for with different  $y$ -offsets from 0 to 0.005 m; the points in blue and red represent calculated data and fitting value for  $B_y$ , and the ones in green and pink represent calculated data and fitting value for  $B_x$ . Note that the nominal position of the extracted beam is at  $x=0$  and  $y=0$  in the new coordinate system.

\* Work supported by DOE under grant No. DE-AC02-76SF00515  
+ zhoufeng@slac.stanford.edu

Table I. Multipole parameters of the QM7R and BS1X.

Multipoles	QM7R	BS1X
$K_0L$	0.008	0.028
$K_1L$	0.3201	$1.155 \times 10^{-3}$
$K_2L$	-26.601	0.34
$K_3L$	$-1.185 \times 10^4$	59.216
$K_4L$	$-3.230 \times 10^6$	$-1.889 \times 10^5$
$K_5L$	$8.205 \times 10^8$	$-1.072 \times 10^9$
$K_6L$	$1.468 \times 10^{12}$	$-1.445 \times 10^{12}$
$K_7L$	$4.527 \times 10^{14}$	$-2.242 \times 10^{15}$
$K_8L$	$-4.316 \times 10^{17}$	$-4.563 \times 10^{18}$
$K_9L$	$-4.456 \times 10^{20}$	$-3.394 \times 10^{21}$

## TRACKING WITH THE MULTIPOLES OF QM7R AND BS1X

### Local Bump Generation

The nominal position of the extracted beam traversing through the QM7R and BS1X is defined at new coordinates system (x, y),  $x=X-0.022$  and  $x=X-0.0855$ , respectively. In the practical beam operations the beam may deviate from the nominal position and experience strong nonlinear field. For the purpose of modeling the beam at different orbits in the extraction channel, local bumps in x- and y-plane are generated, as shown in Fig. 3, by using six correctors including three horizontal and three vertical correctors. Two vertical correctors, ZV9R and ZV1X, and another two horizontal correctors, ZH9R and ZX1X, already exist in the extraction beamline. Other two correctors, horizontal corrector ‘Hadd’ and vertical corrector ‘Vadd’, need to be installed immediate upstream of the QM7R to generate local bumps.

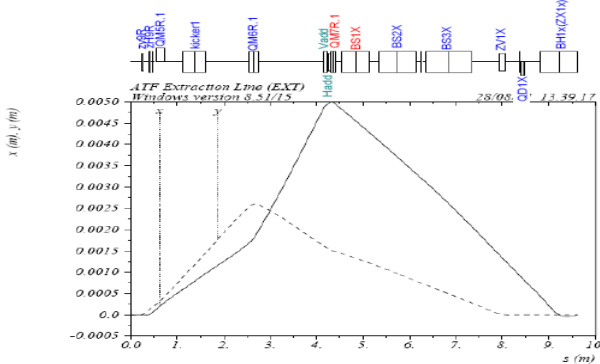


Figure 3: Generation of local bumps in the x- and y-plane in the extraction channel. The bump amplitudes at the QM7R are adjustable by tuning the correctors.

The multi-particle tracking is extensively performed using the MAD program, along the existing beamline starting from the ZV9R in the damping ring to the end of the coupling correction and wire scanners station in the extraction beamline. The following nominal initial parameters are used for the tracking: 5  $\mu\text{m}$  of normalized horizontal emittance, 30 nm of normalized vertical

emittance, 8 mm of bunch length, and 0.08% of the energy spread. The starting Twiss parameter at the ZV9R is exactly taken from the damping ring lattice. At this stage, all magnet errors are not included in this tracking except the multipoles of the QM7R and BS1X. The transverse offset discussed in the next sections is measured at the QM7R in the new coordinate system and the emittance is measured at the end of the extraction beamline.

### Vertical Emittance with X- or Y-offset

Without optics corrections, the normalized vertical emittance vs x- or y-offset from the nominal position without and with multipoles is compared, as shown in Fig. 4. Fig. 4 (right) shows the emittance is significantly increased as y-offset increases and also the emittance growth is dominantly caused by the multipoles while Fig. 4 (left) shows that the vertical emittance keeps constant as x-offset increases.

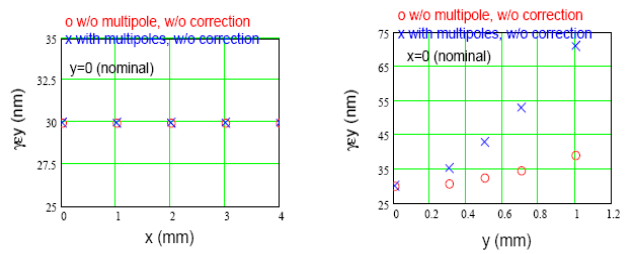


Figure 4: Normalized vertical emittance vs x-offset (left) or y-offset (right) without any optics correction; the results of without and with multipoles are compared.

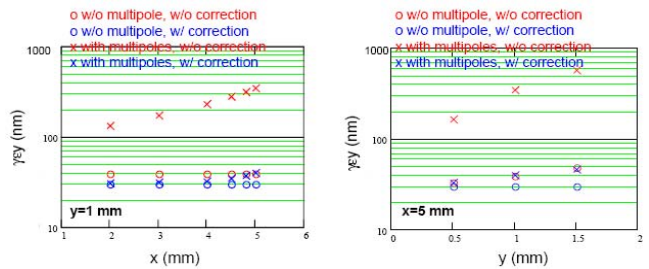


Figure 5: The normalized vertical emittance vs x- and y-offset without and with optics corrections; the results of without and with multipoles are compared.

### Vertical Emittance with X- and Y-offset

Fig. 5 shows the vertical emittance of both x- and y-offset without and with optics corrections for dispersion, coupling and Twiss. The tracking results are also compared for the cases without and with multipoles. For the case without multipoles, shown in Fig. 5 (left), the emittance growth keeps constant at  $y=1$  mm offset since the coupling is not changed, while in Fig. 5 (right) it shows that the emittance is increased as y-offset becomes large. For the case with multipoles, the vertical emittance

is increased by 50% with the offset of  $x=5$  mm and  $y=1.5$  mm even with all optics corrections.

### Transverse Phase Spaces with Beam Offset

The phase spaces of a beam at the nominal position (green), at  $y=1$  mm offset (red) and at  $x=5$  mm offset (brown), are shown in Fig. 6a. It shows that the phase space of  $x=5$  mm offset overlaps closely to the nominal position; this agrees well with the analytical estimate using Hamiltonian [6], while the one with  $y=1$  mm offset blows up, where the beam experiences strong coupling effects. Fig. 6b shows the vertical phase spaces of a beam at the nominal position (green), combined offset of  $x=5$  mm and  $y=1$  mm (red), and  $x=-5$  mm and  $y=1$  mm (brown). It is shown that the phase space volume significantly increases in the offset of  $x=5$  mm and  $y=1$  mm while the one with offset of  $x=-5$  mm and  $y=1$  mm is close to the one at the nominal position. This is because, the magnetic field in the offset of  $x=5$  mm and  $y=1$  mm is in a strong nonlinear region and the one in the offset with  $x=-5$  mm and  $y=1$  mm is in a linear region, which may not dilute the phase space. Figs. 6c and 6d show the phase space  $y-y'$  and  $x-y$  of a beam at the nominal position, combined offset of  $x=5$  mm and  $y=1$  mm without correction (red) and with corrections (brown), respectively. The coupling is corrected well based on the phase space of  $x-y$  (d) in brown, but its corresponding phase space of  $y-y'$  (c) in brown blows up.

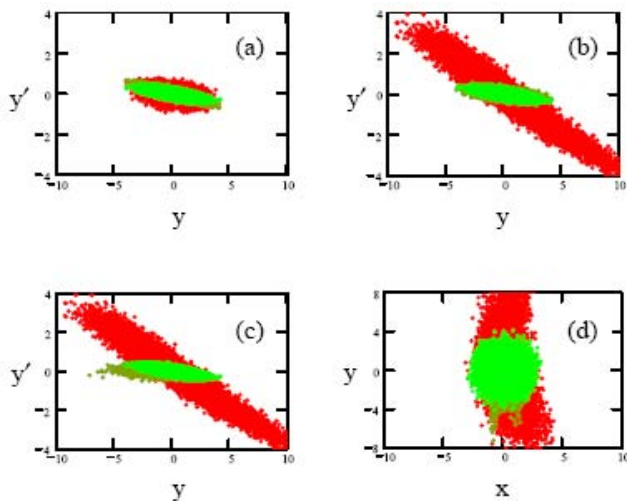


Figure 6: The phase spaces with different transverse offset. The plot (a) corresponds to a beam at the nominal position (green), at  $y=1$  mm offset (red), and at  $x=5$  mm offset (brown); the plot (b) represents a beam at the nominal position (green), at combined  $x=-5$  mm and  $y=1$  mm offset (brown), and combined  $x=5$  mm and  $y=1$  mm offset (red); the plots (c) and (d) show the phase space  $y-y'$  and  $x-y$  of a beam at the nominal position, at combined offset of  $x=5$  mm and  $y=1$  mm without correction (red), and with corrections (brown), respectively.

### Dependence of the Emittance Growth on the Beam Intensity

The strong dependency of vertical emittance growth on the beam intensity was experimentally observed. One of possible reasons to explain the phenomena is that the transverse offsets discussed above are probably created by the transverse wakefield, which depends on the beam intensity. The extensive simulations also indicate that the vertical emittance blows up as the increase of the energy spread, which depends on the beam intensity. Systematic experimental studies are needed to investigate the phenomena.

### Beam Experiment

In order to understand vertical emittance growth source and how well the coupling is corrected using the existing coupling correction setup, beam experiments to measure transverse phase space of an extracted beam traversing through local bumps in the extraction channel is on-going at the existing ATF extraction beamline. Detail results are presented in Ref. [7].

### SUMMARY

The possible source to dilute the vertical emittance at the existing ATF extraction beamline is investigated. The vertical emittance growth is observed in the simulations by changing the beam orbit in the extraction channel, where the magnets are shared by both the ATF damping ring and the extraction beamline, even with all optics corrections turned on. The reasons for the experimentally observed dependence of the vertical emittance growth on the beam intensity are also discussed. An experiment to measure the emittance vs beam orbit at the existing ATF extraction beamline is ongoing led by the European colleagues.

### REFERENCES

- [1] K. Kubo, *et al.*, Extremely low vertical-emittance beam in the Accelerator Test Facility at KEK, *Phys. Rev. Lett.*, 88, 194801 (2002).
- [2] J. Nelson, M. Ross, and M. Woodley, ATF studies, Extraction line dispersion, beam stability and bunch length sensitivity, ATF-2000-06, June 2001.
- [3] S. Kuroda, ATF2 project meeting, March 2007.
- [4] F. Zhou, *et al.*, Simulation studies on the vertical emittance growth at the existing ATF extraction beamline SLAC-PUB-12890, Jan 2008.
- [5] C. M. Spencer, private communication, March 2007.
- [6] S. Kuroda, ATF2 weekly-meeting, June 2007.
- [7] M. Alabau, *et al.*, Study of abnormal vertical emittance growth in ATF extraction line, these proceedings.